

1 **New Axially Chiral Molecular Scaffolds with**
2 **Antibacterial Activities against *Xanthomonas oryzae* pv.**
3 ***oryzae* for Protection of Rice**

4 Yanlin Chen^a, Tingting Li^a, Zhichao Jin^a, Yonggui Robin Chi^{a,b*}

5

6 Address:

7 ^a State Key Laboratory Breeding Base of Green Pesticide and Agricultural
8 Bioengineering, Key Laboratory of Green Pesticide and Agricultural Bioengineering,
9 Ministry of Education, Guizhou University, Huaxi District, Guiyang 550025, China.

10 ^b Division of Chemistry & Biological Chemistry, School of Physical & Mathematical
11 Sciences, Nanyang Technological University, Singapore 637371, Singapore.

12 * Address of the corresponding author

13 E-mail: robinchi@ntu.edu.sg.

14 **ABSTRACT:** A new class of axially chiral thiazine molecules were constructed and
15 showed promising antibacterial activities against plant pathogen *Xanthomonas oryzae*
16 *pv. oryzae* (*Xoo*). The axial chiralities of these compounds (*R* or *S*-atropisomer) showed
17 clear impacts on the *in vitro* inhibitory activities against *Xoo*. An optimal molecule of
18 this class with (*S*)-axially chiral configuration was identified to exhibit inhibitory
19 activity against *Xoo* with an EC₅₀ value of 4.18 µg/mL. This inhibition efficiency is
20 superior to two commercial antibacterial agrochemicals thiodiazole-copper (TC) and
21 bismertiazol (BT) as the positive controls. This hit compound also performed better
22 than the controls in our *in vivo* studies. Preliminary mechanistic studies *via* Scanning
23 Electron Microscopy (SEM) images showed that our hit compound at the concentration
24 of 10 µg/mL destroyed the bacterial integrity of *Xoo*. Label-free quantitative proteomics
25 analysis indicated that a total of 366 differentially expressed proteins of the rice plants
26 were significantly influenced in the presence of our hit molecule.

27 **KEYWORDS:** *axial chirality; thiazine; atropisomer; anti-bacterial; Xoo.*

28 INTRODUCTION

29 The protection of agricultural plants from diseases caused by bacterial infections is an
30 endless battle of both fundamental and practical significance. The problems are often
31 complicated involving many disciplines; and solutions based on physical, biological,
32 and chemical strategies are all used.¹⁻² Each of these strategies has its own merits and
33 limitations, and therefore advancements in all these three domains continue to be
34 critical. In particular, the use of chemicals constitutes a sizable share in modern plant
35 disease management. Many organic molecules and metal compounds, such as
36 azoxystrobin,³ kasugamycin,⁴ and Bordeaux mixture,⁵ have been widely used to treat
37 fungal and / or bacterial infections on various plants.

38 Among these bacterial-related plant diseases, rice bacterial leaf blight caused by
39 *Xanthomonas oryzae* pv. *oryzae* (*Xoo*) remains a most difficult one with potentially big
40 damages.⁶ To date, management of rice bacterial leaf blight is primarily achieved
41 through integration of planting techniques, or with the use of disease resistant rice
42 plants as a most effective manner.⁷⁻⁸ Antimicrobial chemical agents, such as
43 bismertiazol⁹ and Zinc thiazole,¹⁰⁻¹¹ have also been used to control *Xoo* infections.
44 Somewhat unfortunately, the efficacies of these metal or organic chemical agents are
45 largely unsatisfactory as of today.¹²⁻¹³ There is a strong need to search for effective
46 chemical entities to cure or prevent *Xoo* infections on rice plants.

47 Our entry to this problem was directed toward designing new chiral molecules¹⁴
48 for agricultural applications. Agrochemicals containing one or multiple stereocenters
49 (chiral centers) is showing an increasing presence on the markets.¹⁴⁻¹⁶ The enantiomers

50 / stereoisomers often have different efficacies and / or environmental impacts. Typically,
51 one of the two enantiomers (in the case of a racemate) performs better in terms of both
52 efficiency and side effects. Most of these chiral agrochemicals are still used as a mixture
53 of stereoisomers (e.g., racemate of two enantiomers or mixture of multiple
54 diastereomers) to date. On the other hand, with the fast development of chiral synthesis
55 techniques,¹⁷⁻²² one can expect to see commercialization of a bigger number of optically
56 enriched single stereoisomer agrochemicals. It has now well accepted that the
57 development of chiral agrochemicals can significantly contribute to new and greener
58 plant protection solutions. Of the numerous chiral agrochemicals being commercialized
59 or under development, the vast majorities are central-chiral molecules (e.g., molecules
60 with an atom as the stereogenic center) (Figure 1a). In contrast, other types of chiral
61 molecules, such as those based on axial chirality (Figure 1b), are barely explored as
62 pesticides for plant protections.²³⁻²⁷ Axial chirality is a common phenomenon observed
63 in living systems, including natural products isolated from plants.²⁸⁻³¹ Multiple human
64 medicines approved by FDA (U.S. Food and Drug Administration) are racemizing
65 atropisomeric (axially chiral) molecules,³² such as Dabrafenib,³³ Eszopiclone³⁴⁻³⁵ and
66 Afatinib.³⁶⁻³⁷ A much bigger number of axially chiral molecules as potential drug
67 candidates are under active studies at different stages of development.^{32,38-41} The
68 relatively rapid development of axially chiral molecules as human medicines does not
69 seem to influence much of the landscape of the pesticide research field. A representative
70 example of the rather limited studies of axially chiral pesticide is the herbicide
71 Metolachlor (Figure 1b).²⁷ The chiral C-N axis presented in Metolachlor was found to

72 have little influence on the efficacy⁴²⁻⁴³ but different toxicity on aquatic organisms.⁴⁴⁻⁴⁵
73 Other studies of axially chiral molecules as potential pesticides mainly involve isolated
74 natural products bearing chiral axis, such as Laurokamurool and Ustilaginoidin.⁴⁶⁻⁴⁷
75 Overall, very few studies or little background knowledge are available in current
76 literature concerning axially chiral pesticides. There are very few deliberate designs of
77 axially chiral molecules for agricultural uses. Part of the reason, to the best of our
78 understanding, is due to the costs/challenges for access to such axially chiral molecules.
79 On the other hand, in the recent one-to-two decades, with explosive development on
80 asymmetric catalysis and chemical synthesis, synthesis of axially chiral molecules with
81 low cost becomes feasible. We therefore believe that it is now a critical time to start
82 serious evaluation of axially chiral molecules for plant diseases, especially those such
83 as *Xoo* infection that currently does not have an effective chemical solution.

84 Our strategy and key findings are briefed in Figure 1c. We started with two
85 building blocks (**1a** and **2a-m**) that are readily available and contain typical functional
86 moieties found in pesticides and other bioactive molecules. The first building block (**1a**)
87 is an ynol that after reactions become an α,β -unsaturated amide moiety (as in **3a-m**).
88 Similar unsaturated amide groups are found in pesticides such as Maleic hydrazide and
89 Nicobifen.⁴⁸⁻⁵⁰ The second building block (**2a-m**) is an acylated thiourea that after
90 reaction can form a heterocycle (a nitrogen and sulfur atoms-containing thiazine
91 derivative) connecting to multiple heteroatom. Heterocycles of this type are common
92 moieties in bactericides such as Cefradine and Omonasteine. The substituents (R, R',
93 and R'') on both building blocks can be easily modified to offer tunable structures. The

94 two building blocks can react with each other enabled by N-heterocyclic carbene (NHC)
95 organocatalysts studied in our labs and others.⁵¹⁻⁵² Importantly, this organocatalytic
96 reaction (Equation 1) creates a new carbon-nitrogen (C-N) bond as a chiral axis, leading
97 to a novel type of axially chiral molecules (**3a-m**). The axial chirality of most of these
98 molecules (*R* or *S*-atropisomer) shows a clear impact on the *in vitro* inhibitory activities
99 of these molecules against *Xoo*. For example, for a best-performing molecule [*(S)*-**3a**]
100 with *Xoo* inhibition rate at about 92%, the corresponding enantiomer [*(R)*-**3a**] exhibits
101 a much lower inhibition rate at around 52% under otherwise identical experimental
102 conditions (Figure 1c). The EC₅₀ of *(S)*-**3a** (4.18 μg/mL) of the *in vitro* studies is better
103 than those of commercial pesticides (thiodiazole-copper and bismethiazol). This lead
104 compound *(S)*-**3a** also shows promising *in vivo* curative and protective effects on rice
105 plants, compared to blank controls and commercial pesticides. These promising results
106 clearly shows the effects of axial chirality on antimicrobial activities against *Xoo* for
107 rice protection. That information obtained here with this new class of axially chiral
108 molecules is unprecedented, and has potentials for probing new mechanisms of actions.
109 It provides conceptual insights for further explorations of axially chiral molecules for
110 agricultural applications.

111

112 **Figure 1**

113 **MATERIALS AND METHODS**

114 **Instruments and Chemicals.** Commercially available materials were purchased
115 from J&K Scientific and Energy Chemical. NMR spectra were obtained by JEOL-

116 ECX-500 (500 MHz) or Bruker ASCEND 400 (400 MHz) spectrometer. Scanning
117 electron microscope images were observed by Nova Nano SEM 450.

118 **Synthesis of Axially Chiral Compounds (3a-m).**

119 The synthetic scheme (Equation 2) and structures of compounds **3a-m** are
120 illustrated in Figure 2. The synthetic procedures and product characterizations follow
121 a recent report from our own laboratories.⁵³ A typical procedure is as the following.
122 Chiral NHC pre-catalyst (+)-**A** (0.02 mmol, 0.2 equiv., 8.4 mg) was added into a 4.0
123 mL vial equipped with a magnetic stir bar, then DMAP (0.1 mmol, 1.0 equiv., 12.2 mg),
124 Sc(OTf)₃ (0.02 mmol, 0.2 equiv., 9.8 mg), 5 Å molecular sieves (150.0 mg), DQ (0.3
125 mmol, 3.0 equiv., 122.4 mg) and substituted thiourea **2** (0.1 mmol) were added. After
126 that, furan (2.0 mL) and ynal **1a** (0.3 mmol) was added and the reaction mixture was
127 allowed to stir for 12 hours at 30 °C. After consumption of the thiourea substrate **2**, the
128 reaction mixture was directly subjected to column chromatography on silica gel (20:1
129 hexanes / EtOAc) to afford the desired product (*S*)-**3a**. The other enantiomer (*R*)-**3a** was
130 prepared by using the NHC catalyst with the opposite chirality [(-)-**A**] as the catalyst
131 under an otherwise identical condition. The racemic form of the compound [(±)-**3a**]
132 was prepared by using a racemic mixture of the NHC catalyst. Each of the compound
133 were characterized by ¹H, ¹³C, ¹⁹F NMR, as documented in the earlier report.⁵³

134 **Figure 2**

135 **Methods for antibacterial activities against *Xoo*.**

136 The *in vitro* and *in vivo* experiment against *Xoo*, scanning electron microscope
137 analysis and label-free quantitative proteomics analysis were carried out,⁵⁴⁻⁵⁹ and more

138 details could be seen in Supporting Information.

139 **RESULTS AND DISCUSSIONS**

140 **Chemistry**

141 The model axially chiral compounds for antimicrobial activities (**3a-3m**) were
142 readily synthesized from acylthioureas and ynals as the starting materials (Figure 2,
143 Equation 2). The synthesis involves a catalytic one-pot operation developed in our
144 laboratories earlier⁵³. Unlike our previous report⁵³ that concerns new catalysis concept
145 and reaction designs, here in the present study we focused on how the axial chirality
146 and the functional groups presented in the molecules influence the bioactivities. In
147 particular, we introduced different substituent and substitution patterns into the
148 structure of the compound **3** to investigate their antibacterial activities against *Xoo*
149 (Figure 2). Both enantiomers of the target molecules were prepared and evaluated.
150 Substituents commonly found to improve bioactivities in pesticides (such as F, Cl, Br)
151 were found in our study to give high antimicrobial activities against *Xoo* (compound
152 **3a-3c**, **3h**, **3i**). Meanwhile, electron-withdrawing group (NO₂) or electron-donating
153 group (CH₃O) were also installed on the phenyl group to explore the influence of the
154 electronic effect on target compounds (**3d-3f**). Although a comprehensive structure-
155 activity relationship cannot be established at this point, our chemistry designs do
156 provide sufficient insights for further development. For the first time, the chemical
157 entities and their unique spatial arrangements induced by the axial chirality were found
158 to have drastic influence on the antimicrobial activities against *Xoo* that infects rice
159 plants.

160 ***In Vitro* Antibacterial Bioassays.**

161 A series of axially chiral compounds (*R* or *S*-atropisomer) were prepared to
162 investigate the *in vitro* inhibitory activities against *Xoo*. The agricultural antibiotic
163 agents thiodiazole-copper (TC) and bismertiazol (BT) were used as the positive
164 controls. Among the compounds evaluated (Table 1), (*S*)-**3a** was found to exhibit the
165 best antibacterial activity against *Xoo* at the concentrations of 50 and 100 µg/mL. The
166 stereo-configurations (*R*, *S*, *rac*) of the compounds were found to significantly affect
167 their antimicrobial activities. For example, the inhibition rate of (*S*)-**3a** was much better
168 than its enantiomer (*R*)-**3a** and the corresponding racemic mixture [(*rac*)-**3a**].
169 Additional bioactivity studies with (*S*)-**3a** revealed an EC₅₀ value of 4.18 µg/mL, which
170 was superior to those of BT (16.22 µg/mL) and TC (37.35 µg/mL) under the same
171 conditions (Table 1b). Different substituents or substitution patterns also have
172 significant influence on the antibacterial activities of the compounds. For instance,
173 when the Br group of **3a** was moved from the *ortho*- to the *meta*- (**3b**) or *para*-position
174 (**3c**) on the benzene ring of the benzoyl group, a clear decrease on activities were
175 observed. Replacing the *o*-Br group of (*S*)-**3a** with an electron-donating methoxy unit
176 (to get compound **3d**) led to a moderate activity decrease. Multiple other substituents
177 and substitution patterns commonly evaluated for drug and pesticide developments
178 were also studied, as exemplified by compounds **3e-m**. Notably, compound (*S*)-**3e** was
179 found to have an inhibition rate of 53.90% at a concentration of 50 µg/mL and a EC₅₀
180 value of 17.75 µg/mL that is comparable to the positive controls using commercial
181 pesticides (Table 1). As a technical note, as the solubility of these compounds is

182 relatively low in the experimental medium, the observed inhibition rates at the
183 concentrations of 50 and 100 $\mu\text{g}/\text{mL}$ are likely underestimated (Table 1). The EC_{50}
184 values (Table 1b) of the compounds in comparison with the positive controls shall be
185 relatively accurate.

186 **Table 1**

187 ***In Vivo* Bioassay against Rice Bacterial Leaf Blight.**

188 To further evaluate the potential applications of (*S*)-**3a** against rice bacterial leaf
189 blight, *in vivo* experiments were carried out. As shown in Figure 3, (*S*)-**3a** displayed a
190 promising *in vivo* curative activity against this disease with control efficiencies of 45.90%
191 at 200 $\mu\text{g}/\text{mL}$, which was better than that of TC (37.22%). For the protective activity,
192 compound (*S*)-**3a** exerted a control efficiency of 53.70% that was superior to those of
193 BT (20.02%) and TC (47.26%). Results from both *in vitro* and *in vivo* studies suggest
194 that this type of axially chiral thiazine derivatives are a class of new scaffolds worth of
195 further explorations as pesticides to fight against bacterial infections and other plant
196 diseases.

197 **Figure 3**

198 **Scanning Electron Microscopy (SEM).**

199 SEM images were used to detect the morphological variations of pathogens after
200 treatments with compounds (*S*)-**3a** and TC (10 $\mu\text{g}/\text{mL}$, 5 $\mu\text{g}/\text{mL}$) (Figure 4) that
201 expressed in a concentration-dependent manner. The morphology of pathogen *Xoo* was
202 changed from intact to partially damaged or distorted after treatments of (*S*)-**3a** (10
203 $\mu\text{g}/\text{mL}$, 5 $\mu\text{g}/\text{mL}$). Comparing with the positive control (of TC), the morphology of

204 bacteria showed more deformity, corrugations and cracking with the increase of the
205 drug dosages of (S)-**3a**. Observations of the SEM analysis suggested compound (S)-**3a**
206 could cause deformation of the cell membranes for *Xoo*. This disruption of cell
207 membranes likely contributes to (part of) the activities observed from the *in vitro* and
208 *in vivo* studies.

209 **Figure 4**

210 **Label-Free Quantitative Proteomics Analysis.**

211 We obtained a label-free quantitative proteomic profile⁶⁰ by treating rice plant with
212 *Xoo* and compound (S)-**3a** successively (Figure 5), which can derive a preliminary
213 understanding of the adjusting effect and antibacterial mechanism caused by our axially
214 chiral thiazine derivatives. From the rice plant treated with *Xoo* and blank control,
215 approximately 5797 proteins (5620 + 139; Figure 5a) were initially excavated. From
216 the plant treated with *Xoo* and compound (S)-**3a**, the same analysis revealed 5658 (5620
217 + 38) proteins. Among these proteins, 5620 (96.9%) of them were commonly observed
218 from plants treated with blank control and our compound respectively. Comparative
219 proteomic analysis ((S)-**3a**/CK), 366 proteins (97 + 269; Figure 5b) were revealed to be
220 differently expressed when triggered by compound (S)-**3a**. Under the screening
221 conditions of multiple change >1.5 and P < 0.05, 97 proteins were up-regulated and 269
222 proteins were down-regulated.

223 The biological functions of the different expressed proteins were detected by three
224 main GO categories (Figure 5d). The results of Biological Process (BP) analysis
225 showed that these proteins were mainly related to metabolic process, cellular process,

226 biological regulation, localization, and response to stimulus. For the Molecular
227 Function (MF), these proteins were involved in multiple biological actions such as
228 catalytic activity, binding, and transporter activity. Meanwhile, Cellular Component
229 (CC) analysis presented that most of the differentially expressed proteins were
230 concentrated in the cell, the cell part, the organelle and the membrane.

231 Compound (*S*)-**3a** induced different expressions of the multiple proteins, which
232 reveals the reasonable action pathways through the KEGG pathway enrichment bubble
233 plot chart (Figure 5e). Galactose metabolism is one of the main metabolic pathways.
234 It's well known that galactose metabolism plays significant roles in the bioactivities of
235 malate dehydrogenase and isocitrate lyase, which is crucial in multifarious
236 physiological processes incorporating the metabolisms of fat, glucose, and energy. It's
237 also observed that the citrate, malic enzyme, and glyoxylic acid in the glyoxylate and
238 diacid metabolism pathways are down-regulated, which might result in the indirect up-
239 regulation of the Cytochrome P450 that plays significant roles in the nitrogen
240 metabolism pathway. The up-regulation of the Cytochrome P450 can cause the death
241 of the bacteria via improvement of the self-protective ability of the plants. Moreover,
242 the amount of the peroxidase is significantly increased and can strengthen the plant
243 entities to help resist various plant pathogens.

244 **Figure 5**

245 In summary, we have developed a new class of axially chiral thiazine derivatives
246 with antibacterial activities against plant pathogen *Xoo*. Among these molecules,
247 compound (*S*)-**3a** displayed potent inhibition effects with an EC₅₀ value of 4.18 µg/mL

248 that are better than commercial antibacterial agents (BT and TC). *In vivo* studies
249 revealed promising protective activities of (*S*)-**3a** against rice bacterial blight with a
250 control efficiency of 53.70%, which is better than those for BT and TC. The chiralities
251 of these molecules have profound effect on the corresponding antibacterial activities.
252 Preliminary mechanistic studies *via* SEM images showed that the hit compound (*S*)-**3a**
253 could clearly destroy the bacterial integrity of *Xoo*. Label-free quantitative proteomics
254 analysis indicated that a total of 366 proteins were differentially expressed in plant cells
255 as induced by compound (*S*)-**3a**. Our study opens a previously unexplored window in
256 developing axially chiral molecules as effective cures of *Xoo* infections on rice plant.
257 Insights generated from present and future studies in the direction of bioactive axially
258 chiral scaffolds shall likely benefit the area of plant protection beyond *Xoo* infections.
259 Ongoing studies in our laboratories include further structural optimizations and
260 mechanistic evaluations.

261 **AUTHOR INFORMATION**

262 **Corresponding Author**

263 **Yonggui Robin Chi** – *ORCID: 0000-0003-0573-257X*.

264 E-mails: robinchi@ntu.edu.sg.

265 **Authors**

266 **Yanlin Chen** – *ORCID: 0000-0002-5677-4449*.

267 **Tingting Li** – *ORCID: 0000-0003-2657-4646*.

268 **Zhichao Jin** – *ORCID: 0000-0003-3003-6437*.

269 **ACKNOWLEDGMENTS**

270 We acknowledge financial support from the National Natural Science Foundation of
271 China (21772029, 32172459, 21961006, 22071036), The 10 Talent Plan (Shicengci) of
272 Guizhou Province ([2016]5649), the Science and Technology Department of Guizhou
273 Province ([2019]1020, Qiankehejichu-ZK[2021]Key033), the Program of Introducing
274 Talents of Discipline to Universities of China (111 Program, D20023) at Guizhou
275 University, Frontiers Science Center for Asymmetric Synthesis and Medicinal
276 Molecules, Department of Education, Guizhou Province [Qianjiaohe KY (2020)004],
277 the Guizhou Province First-Class Disciplines Project [(Yiliu Xueke Jianshe Xiangmu)-
278 GNYL(2017)008], Guizhou University of Traditional Chinese Medicine, and Guizhou
279 University (China). Singapore National Research Foundation under its NRF
280 Investigatorship (NRF-NRFI2016-06) and Competitive Research Program (NRF-
281 CRP22-2019-0002); the Ministry of Education, Singapore, under its MOE AcRF Tier
282 1 Award (RG7/20, RG5/19), MOE AcRF Tier 2 (MOE2019-T2-2-117), MOE AcRF
283 Tier 3 Award (MOE2018-T3-1-003); Nanyang Research Award Grant, Chair
284 Professorship Grant, Nanyang Technological University.

285 **Notes**

286 The authors confirm that this article content has no conflict of interest.

287 **ABBREVIATIONS**

288 *Xoo*, *Xanthomonas oryzae* pv. *oryzae*; SDS-PAGE, sodium dodecyl sulfate-
289 polyacrylamide gel electrophoresis; EC₅₀, the half maximal effective concentrations;
290 TC, Thiodiazole copper; BT, bismertiazol; DMAP, 4-Dimethylaminopyridine; SEM,
291 Scanning Electron Microscopy.

292 **REFERENCES**

- 293 (1) Azizbekyan, R. R. Biological preparations for the protection of agricultural plants
294 (Review). *Appl. Biochem. Microbiol.* **2019**, *55* (8), 816-823.
- 295 (2) Ragsdale, N. N. The role of pesticides in agricultural crop protection. *Ann. N.Y. Acad.*
296 *Sci.* **1999**, *894*, 199-205.
- 297 (3) Rodrigues, E. T.; Lopes, I.; Pardal, M. A. Occurrence, fate and effects of
298 azoxystrobin in aquatic ecosystems: A review. *Environ. Int.* **2013**, *53*, 18-28.
- 299 (4) Levitan, A. A. In vitro antibacterial activity of kasugamycin. *Appl. Microbiol.* **1967**,
300 *15* (4), 750-753.
- 301 (5) Gutierrez-Barranquero, J. A.; Arrebola, E.; Bonilla, N.; Sarmiento, D.; Cazorla, F.
302 M.; de Vicente, A. Environmentally friendly treatment alternatives to Bordeaux mixture
303 for controlling bacterial apical necrosis (BAN) of mango. *Plant Pathol.* **2012**, *61* (4),
304 665-676.
- 305 (6) Mew, T. W. Focus on bacterial blight of rice. *Plant Dis.* **1993**, *77* (1), 5-12.
- 306 (7) Chukwu, S. C.; Rafii, M. Y.; Ramlee, S. I.; Ismail, S. I.; Hasan, M. M.; Oladosu, Y.
307 A.; Magaji, U. G.; Akos, I.; Olalekan, K. K. Bacterial leaf blight resistance in rice: a
308 review of conventional breeding to molecular approach. *Mol. Biol. Rep.* **2019**, *46* (1),
309 1519-1532.
- 310 (8) Fred, A. K.; Kiswara, G.; Yi, G.; Kim, K.-M. Screening rice cultivars for resistance
311 to bacterial leaf blight. *J. Microbiol. Biotechnol.* **2016**, *26* (5), 938-945.
- 312 (9) Zhu, X.-F.; Xu, Y.; Peng, D.; Zhang, Y.; Huang, T.-T.; Wang, J.-X.; Zhou, M.-G.
313 Detection and characterization of bismertiazol-resistance of *Xanthomonas oryzae* pv.

314 *oryzae*. *Crop Protect.* **2013**, *47*, 24-29.

315 (10) Zhang, C.; Wu, H.; Li, X.; Shi, H.; Wei, F.; Zhu, G. Baseline sensitivity of natural
316 populations and resistance of mutants of *Xanthomonas oryzae* pv. *oryzae* to a novel
317 bactericide, zinc thiazole. *Plant Pathol.* **2013**, *62* (6), 1378-1383.

318 (11) Chen, Y.; Yang, X.; Gu, C. Y.; Zhang, A. F.; Zhang, Y.; Wang, W. X.; Gao, T. C.;
319 Yao, J.; Yuan, S. K. Activity of a novel bactericide, zinc thiazole against *Xanthomonas*
320 *oryzae* pv. *oryzae* in Anhui Province of China. *Ann. Appl. Biol.* **2015**, *166* (1), 129-135.

321 (12) Shen, Y.; Ronald, P. Molecular determinants of disease and resistance in
322 interactions of *Xanthomonas oryzae* pv. *oryzae* and rice. *Microb. Infect.* **2002**, *4* (13),
323 1361-1367.

324 (13) Zhang, Y.; Pan, X.; Duan, Y.; Zhu, X.; Ma, X.; Huang, T.; Gao, T.; Zhou, M. The
325 screening of bismertiazol-resistant genes in *Xanthomonas oryzae* pv. *oryzae*.
326 *Australas. Plant Pathol.* **2015**, *44* (5), 541-543.

327 (14) Jeschke, P. Current status of chirality in agrochemicals. *Pest Manage. Sci.* **2018**,
328 *74* (11), 2389-2404.

329 (15) Sasaki, M. Current status of organophosphorus insecticide and stereochemistry.
330 *Phosphorus, Sulfur Silicon Relat. Elem.* **2008**, *183* (2-3), 291-299.

331 (16) Liu, W.; Ye, J.; Jin, M. Enantioselective phytoeffects of chiral pesticides. *J. Agric.*
332 *Food Chem.* **2009**, *57* (6), 2087-2095.

333 (17) Brak, K.; Jacobsen, E. N. Asymmetric ion-pairing catalysis. *Angew. Chem. Int. Ed.*
334 **2013**, *52* (2), 534-561.

335 (18) Gu, Z.-G.; Zhan, C.; Zhang, J.; Bu, X. Chiral chemistry of metal-camphorate

336 frameworks. *Chem. Soc. Rev.* **2016**, *45* (11), 3122-3144.

337 (19) Gao, D.-W.; Gu, Q.; Zheng, C.; You, S.-L. Synthesis of planar chiral ferrocenes
338 via transition-metal-catalyzed direct C-H bond functionalization. *Acc. Chem. Res.* **2017**,
339 *50* (2), 351-365.

340 (20) Xue, Y.-P.; Cao, C.-H.; Zheng, Y.-G. Enzymatic asymmetric synthesis of chiral
341 amino acids. *Chem. Soc. Rev.* **2018**, *47* (4), 1516-1561.

342 (21) Cheng, J. K.; Xiang, S.-H.; Li, S.; Ye, L.; Tan, B. Recent advances in catalytic
343 asymmetric construction of atropisomers. *Chem. Rev.* **2021**, *121* (8), 4805-4902.

344 (22) Kitagawa, O. Chiral Pd-catalyzed enantioselective syntheses of various N-C
345 axially chiral compounds and their synthetic applications. *Acc. Chem. Res.* **2021**, *54* (3),
346 719-730.

347 (23) Mueller, M. D.; Buser, H. R. Environmental behavior of acetamide pesticide
348 stereoisomers. 2. Stereo- and enantioselective degradation in sewage sludge and soil.
349 *Environ. Sci. Technol.* **1995**, *29* (8), 2031-2037.

350 (24) Eish, M. Y. Z. A.; Wells, M. J. M. Monitoring stereoselective degradation of
351 metolachlor in a constructed wetland: Use of statistically valid enantiomeric and
352 diastereomeric fractions as opposed to ratios. *J. Chromatogr. Sci.* **2008**, *46* (3), 269-275.

353 (25) Liu, Y.; Zhang, X.; Liu, C.; Yang, R.; Xu, Z.; Zhou, L.; Sun, Y.; Lei, H.
354 Enantioselective and synergetic toxicity of axial chiral herbicide propisochlor to SP2/0
355 myeloma cells. *J. Agric. Food Chem.* **2015**, *63* (36), 7914-7920.

356 (26) Li, T.-X.; Yang, M.-H.; Wang, Y.; Wang, X.-B.; Luo, J.; Luo, J.-G.; Kong, L.-Y.
357 Unusual dimeric tetrahydroxanthone derivatives from *Aspergillus lentulus* and the

358 determination of their axial chiralities. *Sci. Rep.* **2016**, *6*, 38958.

359 (27) Xie, J.; Zhao, L.; Liu, K.; Guo, F.; Liu, W. Enantioseparation of four amide
360 herbicide stereoisomers using high-performance liquid chromatography. *J. Chromatogr.*
361 *A* **2016**, *1471*, 145-154.

362 (28) Yu, S.; Ma, S. Allenes in catalytic asymmetric synthesis and natural product
363 syntheses. *Angew. Chem. Int. Ed.* **2012**, *51* (13), 3074-3112.

364 (29) Toenjes, S. T.; Gustafson, J. L. Atropisomerism in medicinal chemistry: challenges
365 and opportunities. *Future Med. Chem.* **2018**, *10* (4), 409-422.

366 (30) Huang, X.; Ma, S. Alienation of terminal alkynes with aldehydes and ketones. *Acc.*
367 *Chem. Res.* **2019**, *52* (5), 1301-1312.

368 (31) Tajuddeen, N.; Bringmann, G. N,C-Coupled naphthylisoquinoline alkaloids: a
369 versatile new class of axially chiral natural products. *Nat. Prod. Rep.* **2021**,
370 DOI:10.1039/D1NP00020A.

371 (32) Toenjes, S. T.; Gustafson, J. L. Atropisomerism in medicinal chemistry: challenges
372 and opportunities. *Future Med. Chem.* **2018**, *10* (4), 409-422.

373 (33) Jung, B.; Kim, J.; Bae, J.-S. Dabrafenib, as a novel insight into drug repositioning
374 against secretory group IIa phospholipase A2. *Int. J. Pharmacol.* **2016**, *12* (4), 415-421.

375 (34) Hair, P. I.; McCormack, P. L.; Curran, M. P. Eszopiclone - A review of its use in
376 the treatment of insomnia. *Drugs* **2008**, *68* (10), 1415-1434.

377 (35) Doerr, J. P.; Riemann, D. Treating insomnia with eszopiclone.
378 *Psychopharmakotherapie* **2009**, *16* (5), 186.

379 (36) Liao, B. C.; Lin, C. C.; Yang, J. C. Novel EGFR Inhibitors in Non-small Cell Lung

380 Cancer: Current Status of Afatinib. *Curr. Oncol. Rep.* **2017**, *19* (1), 4.

381 (37) Shi, Y.; Wang, M. Afatinib as first-line treatment for advanced lung
382 adenocarcinoma patients harboring HER2 mutation: A case report and review of the
383 literature. *Thorac. Cancer* **2018**, *9* (12), 1788-1794.

384 (38) Welch, W. M.; Ewing, F. E.; Huang, J.; Menniti, F. S.; Pagnozzi, M. J.; Kelly, K.;
385 Seymour, P. A.; Guanowsky, V.; Guhan, S.; Guinn, M. R.; Critchett, D.; Lazzaro, J.;
386 Ganong, A. H.; DeVries, K. M.; Staigers, T. L.; Chenard, B. L. Atropisomeric
387 quinazolin-4-one derivatives are potent noncompetitive α -amino-3-hydroxy-5-methyl-
388 4-isoxazolepropionic acid (AMPA) receptor antagonists. *Bioorg. Med. Chem. Lett.*
389 **2001**, *11* (2), 177-181.

390 (39) Sugane, T.; Tobe, T.; Hamaguchi, W.; Shimada, I.; Maeno, K.; Miyata, J.; Suzuki,
391 T.; Kimizuka, T.; Sakamoto, S.; Tsukamoto, S. Atropisomeric 4-phenyl-4*H*-1,2,4-
392 triazoles as selective glycine transporter 1 inhibitors. *J. Med. Chem.* **2013**, *56* (14),
393 5744-56.

394 (40) De Lucca, G. V.; Shi, Q.; Liu, Q.; Batt, D. G.; Beaudoin Bertrand, M.; Rampulla,
395 R.; Mathur, A.; Discenza, L.; D'Arienzo, C.; Dai, J.; Obermeier, M.; Vickery, R.; Zhang,
396 Y.; Yang, Z.; Marathe, P.; Tebben, A. J.; Muckelbauer, J. K.; Chang, C. J.; Zhang, H.;
397 Gillooly, K.; Taylor, T.; Pattoli, M. A.; Skala, S.; Kukral, D. W.; McIntyre, K. W.; Salter-
398 Cid, L.; Fura, A.; Burke, J. R.; Barrish, J. C.; Carter, P. H.; Tino, J. A. Small molecule
399 reversible inhibitors of Bruton's Tyrosine Kinase (BTK): structure-activity relationships
400 leading to the identification of 7-(2-Hydroxypropan-2-yl)-4-[2-methyl-3-(4-oxo-3,4-
401 dihydroquinazolin-3-yl)phenyl]-9*H*-carbazole-1-carboxamide (BMS-935177). *J. Med.*

402 *Chem.* **2016**, *59* (17), 7915-35.

403 (41) Watterson, S. H.; De Lucca, G. V.; Shi, Q.; Langevine, C. M.; Liu, Q.; Batt, D. G.;
404 Beaudoin Bertrand, M.; Gong, H.; Dai, J.; Yip, S.; Li, P.; Sun, D.; Wu, D. R.; Wang, C.;
405 Zhang, Y.; Traeger, S. C.; Pattoli, M. A.; Skala, S.; Cheng, L.; Obermeier, M. T.; Vickery,
406 R.; Discenza, L. N.; D'Arienzo, C. J.; Zhang, Y.; Heimrich, E.; Gillooly, K. M.; Taylor,
407 T. L.; Pulicicchio, C.; McIntyre, K. W.; Galella, M. A.; Tebben, A. J.; Muckelbauer, J.
408 K.; Chang, C.; Rampulla, R.; Mathur, A.; Salter-Cid, L.; Barrish, J. C.; Carter, P. H.;
409 Fura, A.; Burke, J. R.; Tino, J. A. Discovery of 6-fluoro-5-(*R*)-(3-(*S*)-(8-fluoro-1-
410 methyl-2,4-dioxo-1,2-dihydroquinazolin-3(*H*)-yl)-2-methylphenyl)-2-(*S*)-(2-
411 hydroxypropan-2-yl)-2,3,4,9-tetrahydro-1*H*-carbazole-8-carboxamide (BMS-986142):
412 a reversible inhibitor of Bruton's Tyrosine Kinase (BTK) conformationally constrained
413 by two locked atropisomers. *J. Med. Chem.* **2016**, *59* (19), 9173-9200.

414 (42) Ye, J.; Wu, J.; Liu, W. Enantioselective separation and analysis of chiral pesticides
415 by high-performance liquid chromatography. *TrAC, Trends Anal. Chem.* **2009**, *28* (10),
416 1148-1163.

417 (43) Ye, J.; Zhao, M.; Niu, L.; Liu, W. Enantioselective environmental toxicology of
418 chiral pesticides. *Chem. Res. Toxicol.* **2015**, *28* (3), 325-338.

419 (44) Liu, Y.; Zhang, X.; Liu, C.; Yang, R.; Xu, Z.; Zhou, L.; Sun, Y.; Lei, H.
420 Enantioselective and synergetic toxicity of axial chiral herbicide propisochlor to SP2/0
421 myeloma Cells. *J. Agric. Food Chem.* **2015**, *63* (36), 7914-7920.

422 (45) Chen, S.; Zhang, L.; Chen, H.; Chen, Z.; Wen, Y. Enantioselective toxicity of chiral
423 herbicide Metolachlor to *Microcystis aeruginosa*. *J. Agric. Food Chem.* **2019**, *67* (6),

424 1631-1637.

425 (46) Li, X. L.; Kurtan, T.; Hu, J. C.; Mandi, A.; Li, J.; Li, X. W.; Guo, Y. W. Structural
426 and stereochemical studies of Laurokamurols A-C, uncommon bis-sesquiterpenoids
427 from the Chinese Red Alga *Laurencia Okamurai* Yamada. *J. Agric. Food Chem.* **2017**,
428 *65* (8), 1550-1555.

429 (47) Sun, W.; Wang, A.; Xu, D.; Wang, W.; Meng, J.; Dai, J.; Liu, Y.; Lai, D.; Zhou, L.
430 New ustilaginoidins from rice false smut balls caused by *villosiclava virens* and their
431 phytotoxic and cytotoxic activities. *J. Agric. Food Chem.* **2017**, *65* (25), 5151-5160.

432 (48) Leopold, A. C.; Klein, W. H. Maleic hydrazide as an antiauxin in plants. *Science*
433 **1951**, *114* (2949), 9-10.

434 (49) Strunz, G. M.; Finlay, H. Concise, efficient new synthesis of pipericide, an
435 insecticide unsaturated amide from piper-nigrum, and related-compounds. *Tetrahedron*
436 **1994**, *50* (38), 11113-11122.

437 (50) Walker, S. B. Common names of pesticides recently approved by the BSI. *Pest*
438 *Manag. Sci.* **2003**, *59* (3), 371-373.

439 (51) Maiti, R.; Xu, J.; Yan, J.-L.; Mondal, B.; Yang, X.; Chai, H.; Hao, L.; Jin, Z.; Chi,
440 Y. R. Carbene-catalyzed selective addition of isothioureas to enals for access to sulphur-
441 containing 5,6-dihydropyrimidin-4-ones. *Org. Chem. Front.* **2021**, *8* (4), 743-747.

442 (52) Cao, L.; Li, T.; Chi, Y. R.; Jin, Z. Carbene-catalyzed *N,N*-nucleophilic activation
443 of thioureas for access to pyrimidinthione derivatives. *Asian J. Org. Chem.* **2021**, *10*
444 (5), 1090-1093.

445 (53) Li, T.; Mou, C.; Qi, P.; Peng, X.; Jiang, S.; Hao, G.; Xue, W.; Yang, S.; Hao, L.;

446 Chi, Y. R.; Jin, Z. *N*-Heterocyclic carbene-catalyzed atroposelective annulation for
447 access to thiazine derivatives with C-N axial chirality. *Angew. Chem. Int. Ed.* **2021**, *60*
448 (17), 9362-9367.

449 (54) Li, P.; Tian, P.; Chen, Y.; Song, X.; Xue, W.; Jin, L.; Hu, D.; Yang, S.; Song, B.
450 Novel bithioether derivatives containing a 1,3,4-oxadiazole moiety: design, synthesis,
451 antibacterial and nematocidal activities. *Pest Manag. Sci.* **2018**, *74* (4), 844-852.

452 (55) Tao, Q.-Q.; Liu, L.-W.; Wang, P.-Y.; Long, Q.-S.; Zhao, Y.-L.; Jin, L.-H.; Xu, W.-
453 M.; Chen, Y.; Li, Z.; Yang, S. Synthesis and *in vitro* and *in vivo* biological activity
454 evaluation and quantitative proteome profiling of oxadiazoles bearing flexible
455 heterocyclic patterns. *J. Agric. Food Chem.* **2019**, *67* (27), 7626-7639.

456 (56) Wang, P.; Wang, M.; Zeng, D.; Xiang, M.; Rao, J. R.; Liu, Q.; Liu, L.; Wu, Z.; Li,
457 Z.; Song, B.; Yang, S. Rational optimization and action mechanism of novel imidazole
458 (or imidazolium)-labeled 1,3,4-oxadiazole thioethers as promising antibacterial agents
459 against plant bacterial diseases. *J. Agric. Food Chem.* **2019**, *67* (13), 3535-3545.

460 (57) Zhao, Y.-L.; Huang, X.; Liu, L.-W.; Wang, P.-Y.; Long, Q.-S.; Tao, Q.-Q.; Li, Z.;
461 Yang, S. Identification of racemic and chiral carbazole derivatives containing an
462 isopropanolamine linker as prospective surrogates against plant pathogenic bacteria: *in*
463 *vitro* and *in vivo* assays and quantitative proteomics. *J. Agric. Food Chem.* **2019**, *67*
464 (26), 7512-7525.

465 (58) Ni, H.; Pan, W.; Jin, Q.; Xie, Y.; Zhang, N.; Chen, K.; Lin, T.; Lin, C.; Xie, Y.; Wu,
466 J.; Ni, P.; Wu, L. Label-free proteomic analysis of serum exosomes from paroxysmal
467 atrial fibrillation patients. *Clin. Proteomics* **2021**, *18* (1), 1.

- 468 (59) Liang, X.; Guan, H.; Sun, J.; Qi, Y.; Yao, W. Comparative proteomic analysis of
469 tPVAT during a Ang II infusion. *Biomedicines* **2021**, *9* (12), 1820.
- 470 (60) Matros, A.; Kaspar, S.; Witzel, K.; Mock, H. P. Recent progress in liquid
471 chromatography-based separation and label-free quantitative plant proteomics.
472 *Phytochemistry* **2011**, *72* (10), 963-974.

473 **Figure Captions**

474 **Figure 1** Designing new axially chiral molecule scaffolds for potential treatment of rice
475 plant *Xoo* infections.

476 **Figure 2** Synthesis and structures of the axially chiral molecules.

477 **Figure 3** Curative and protective activities of (*S*)-**3a** against rice bacterial blight at 200
478 $\mu\text{g/mL}$. BT and TC were the positive controls.

479 **Figure 4** SEM images for *Xoo* after incubation in various dosages of (*S*)-**3a** or
480 thiodiazole-copper. (*S*)-**3a**: (a) 0 $\mu\text{g/mL}$, (b) 10 $\mu\text{g/mL}$, (c) 5 $\mu\text{g/mL}$; thiodiazole-copper:
481 (d) 10 $\mu\text{g/mL}$, (e) 5 $\mu\text{g/mL}$. Scale bars for (a)–(e) are 2000 nm.

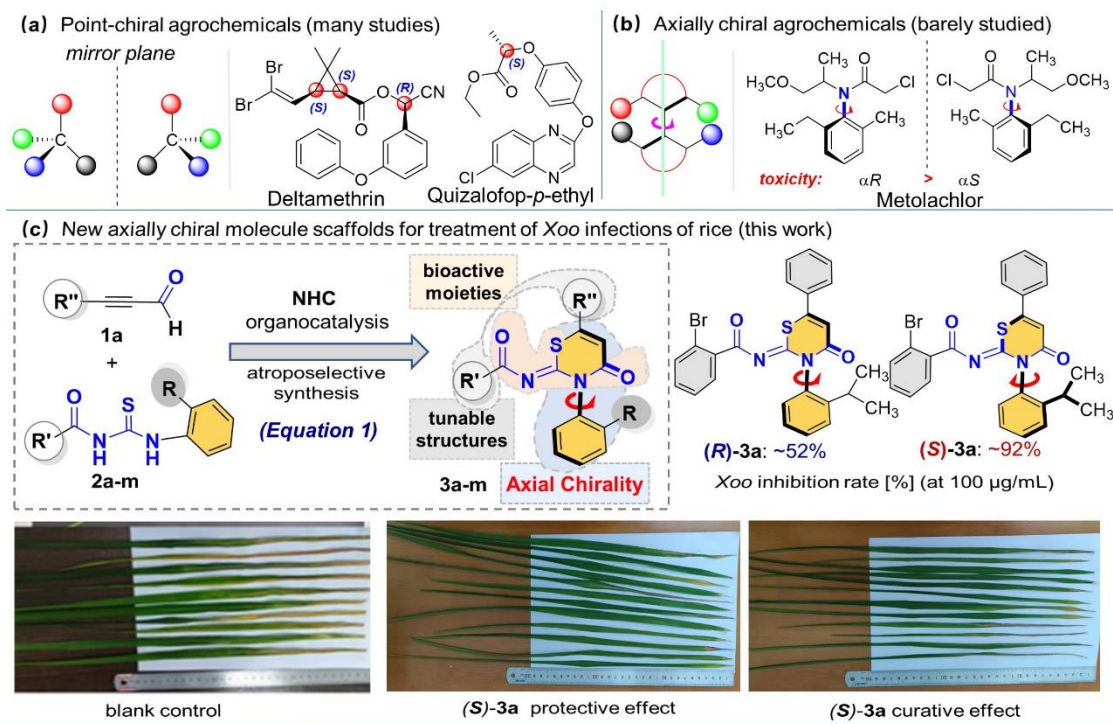
482 **Figure 5** (a) Venn diagrams for proteome comparison on control and treatment groups;
483 (b) histogram of the number distribution of differentially expressed proteins in different
484 comparison groups [(*S*)-**3a**/CK]; (c) volcano plot of differentially expressed proteins
485 [(*S*)-**3a**/CK]; (d) Differentially expressed proteins in control and treatment groups; (e)
486 KEGG pathway enrichment bubble plot of differentially expressed proteins

Table 1 *In vitro* antibacterial activities of title compounds against pathogens *Xoo*(a) Preliminary antibacterial activities of title compounds against pathogens *Xoo in Vitro*

Compounds	Xoo inhibition rate [%]		Compounds	Xoo inhibition rate [%]	
	100 µg/mL	50 µg/mL		100 µg/mL	50 µg/mL
(<i>R</i>)- 3a	52.25 ± 5.57	28.87 ± 8.01	(<i>R</i>)- 3h	9.04 ± 9.09	14.04 ± 5.51
(<i>S</i>)- 3a	92.16 ± 9.38	58.91 ± 3.61	(<i>S</i>)- 3h	35.02 ± 7.57	18.41 ± 3.12
(<i>rac</i>)- 3a	70.18 ± 7.67	31.52 ± 5.45	(<i>rac</i>)- 3h	20.18 ± 1.68	11.64 ± 3.18
(<i>R</i>)- 3b	37.96 ± 2.86	32.67 ± 8.21	(<i>R</i>)- 3i	44.26 ± 7.51	7.65 ± 3.59
(<i>S</i>)- 3b	18.28 ± 9.15	2.95 ± 9.73	(<i>S</i>)- 3i	47.16 ± 8.84	31.43 ± 2.37
(<i>rac</i>)- 3b	77.33 ± 1.62	46.06 ± 3.69	(<i>rac</i>)- 3i	19.28 ± 5.30	36.27 ± 3.64
(<i>R</i>)- 3c	25.83 ± 3.51	4.40 ± 2.47	(<i>R</i>)- 3j	47.85 ± 1.55	21.11 ± 2.21
(<i>S</i>)- 3c	34.07 ± 3.58	15.84 ± 7.24	(<i>S</i>)- 3j	68.28 ± 8.15	32.95 ± 4.73
(<i>rac</i>)- 3c	31.57 ± 9.16	26.77 ± 6.18	(<i>rac</i>)- 3j	51.33 ± 2.62	16.06 ± 3.69
(<i>R</i>)- 3d	74.28 ± 5.44	23.88 ± 4.76	(<i>R</i>)- 3k	46.47 ± 9.54	5.65 ± 4.84
(<i>S</i>)- 3d	86.76 ± 2.62	47.00 ± 1.90	(<i>S</i>)- 3k	39.73 ± 8.59	9.95 ± 3.96
(<i>rac</i>)- 3d	42.01 ± 3.92	34.47 ± 2.67	(<i>rac</i>)- 3k	13.63 ± 6.98	4.17 ± 2.08
(<i>R</i>)- 3e	54.75 ± 4.71	23.78 ± 4.39	(<i>R</i>)- 3l	37.39 ± 0.68	15.83 ± 9.19
(<i>S</i>)- 3e	68.23 ± 5.38	53.90 ± 2.29	(<i>S</i>)- 3l	45.56 ± 4.47	15.97 ± 7.46
(<i>rac</i>)- 3e	65.48 ± 2.78	62.19 ± 6.42	(<i>rac</i>)- 3l	18.32 ± 6.52	27.25 ± 3.15
(<i>R</i>)- 3f	44.96 ± 7.32	25.42 ± 1.65	(<i>R</i>)- 3m	32.47 ± 9.57	23.08 ± 6.54
(<i>S</i>)- 3f	37.96 ± 1.95	37.11 ± 4.14	(<i>S</i>)- 3m	38.11 ± 6.59	34.42 ± 3.20
(<i>rac</i>)- 3f	40.56 ± 9.94	36.11 ± 1.65	(<i>rac</i>)- 3m	22.58 ± 9.02	11.54 ± 2.33
(<i>R</i>)- 3g	28.72 ± 2.34	17.78 ± 1.59	TC	87.79 ± 4.69	53.45 ± 2.11
(<i>S</i>)- 3g	17.48 ± 3.70	19.88 ± 8.26	BT	98.30 ± 2.19	79.53 ± 1.11
(<i>rac</i>)- 3g	21.88 ± 1.23	18.11 ± 5.11	/	/	/

(b) EC₅₀ values of target compounds(*S*)-**3a**, (*S*)-**3d** and (*S*)-**3e** against *Xoo*

Compounds	Xoo inhibition rate [%]		
	regression equation	EC ₅₀ (µg/mL)	R ²
(<i>S</i>)- 3a	y = 0.5285x + 4.6729	4.18	0.9257
(<i>S</i>)- 3d	y = 0.4730x + 4.1628	58.88	0.9165
(<i>S</i>)- 3e	y = 0.9932x + 3.7594	17.75	0.9677
BT	y = 2.5275x + 1.9419	16.22	0.9514
TC	y = 0.4267x + 4.3291	37.35	0.9758

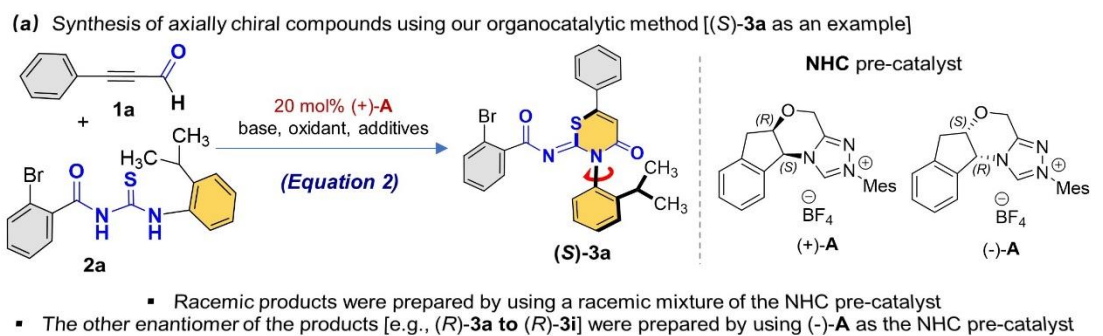


489

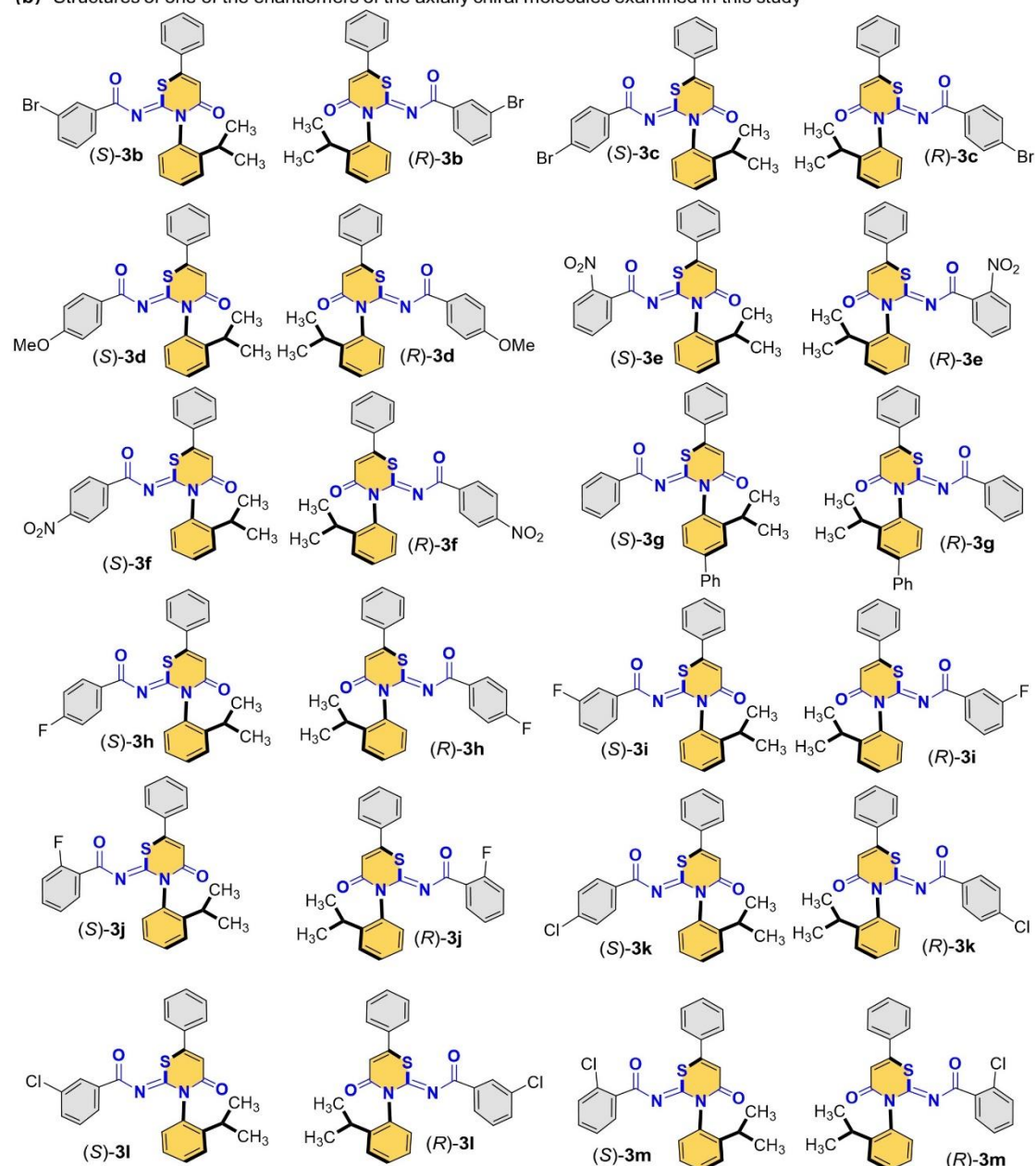
490 **Figure 1** Designing new axially chiral molecule scaffolds for potential treatment of rice plant *Xoo*

491 infections.

492



(b) Structures of one of the enantiomers of the axially chiral molecules examined in this study



493

494 **Figure 2** Synthesis and structures of the axially chiral molecules.

495

Compounds	Morbidity(%)	Curative activity (14 day after spraying)		Protective activity (14 day after spraying)	
		disease index	control efficiency(%) ^b	disease index	control efficiency(%) ^b
(S)-3a	100	45.80	45.90	39.20	53.70
TC	100	53.17	37.22	67.74	20.02
BT	100	36.67	56.71	44.67	47.26
CK ^a	100	84.70	/	84.70	/

^a Negative control. ^b Statistical analysis was conducted by the ANOVA method under the condition of equal variances assumed ($P > 0.05$) and equal variances not assumed ($P < 0.05$).



496

497 **Figure 3** Curative and protective activities of (S)-3a against rice bacterial blight at 200

498 $\mu\text{g/mL}$. BT and TC were the positive controls.

499



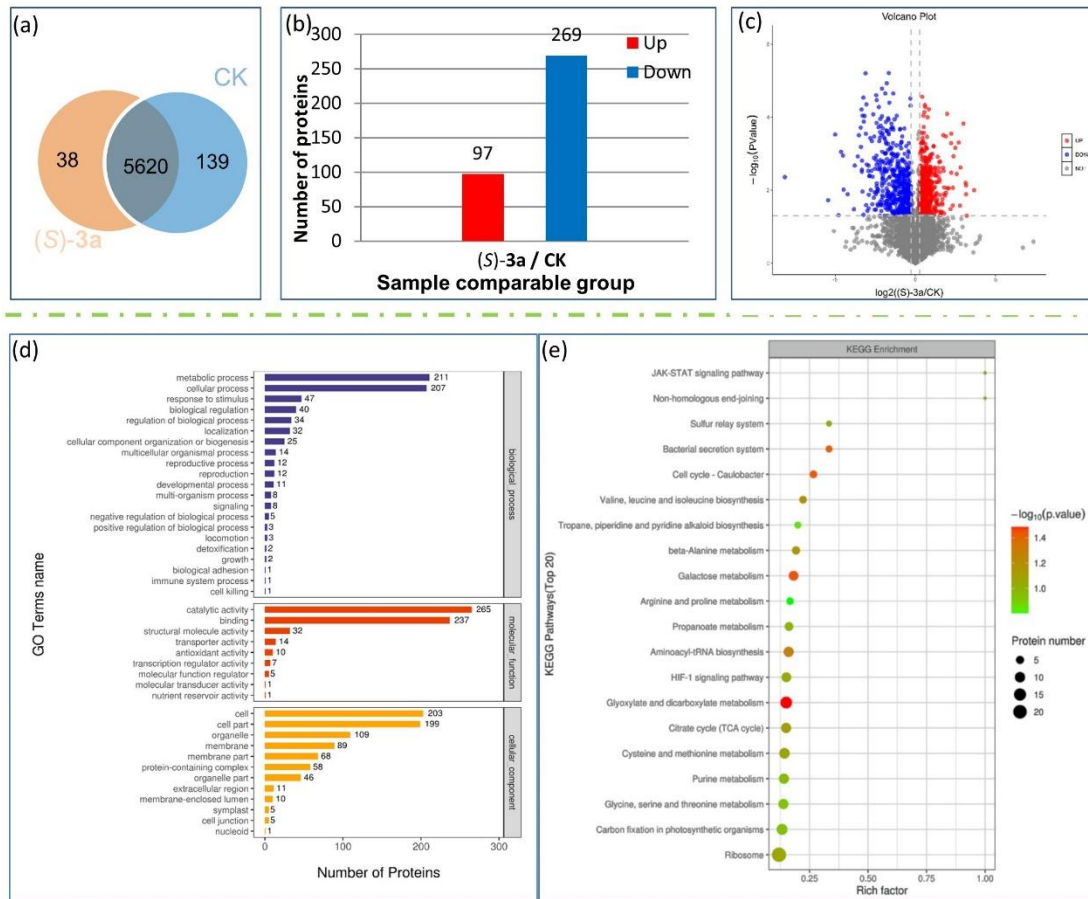
500

501 **Figure 4** SEM images for *Xoo* after incubation in various dosages of (*S*)-**3a** or

502 thiodiazole-copper. (*S*)-**3a**: (a) 0 µg/mL, (b) 10 µg/mL, (c) 5 µg/mL; thiodiazole-copper:

503 (d) 10 µg/mL, (e) 5 µg/mL. Scale bars for (a)–(e) are 2000 nm.

504



505

506 **Figure 5** (a) Venn diagrams for proteome comparison on control and treatment groups;

507 (b) histogram of the number distribution of differentially expressed proteins in different

508 comparison groups [(S)-3a/CK]; (c) volcano plot of differentially expressed proteins

509 [(S)-3a/CK]; (d) Differentially expressed proteins in control and treatment groups; (e)

510 KEGG pathway enrichment bubble plot of differentially expressed proteins.

511 TOC Graphic:

